JOURNAL OF CATALYSIS 115, 365–375 (1989)

The Effect of a Coverage-Dependent Heat of Adsorption on Temperature-Programmed Desorption and Adsorption in Porous Catalysts

A. R. BALKENENDE, J. W. GEUS, A. J. H. M. KOCK,[1] AND R. J. VAN DER PAS[2]

Department of Inorganic Chemistry, University of Utrecht, Croesestraat 77A, 3522 AD Utrecht, The Netherlands

Received August 10, 1987; revised April 14, 1988

A model describing adsorption and desorption in a bed of porous catalyst pellets is presented. The model has been used to simulate temperature-programmed desorption. In particular the effect of a coverage-dependent heat of adsorption has been investigated and the consequences thereof for commonly used interpretation methods are shown. It appears that the method in which the heating rate is varied and the method using desorption rate isotherms yield values which roughly approach the heat of adsorption used for the calculation of the desorption profiles in the case of the coverage-dependent heat of adsorption. Adsorption experiments, either in a flow of adsorbate or under static conditions, have also been simulated. If the net rate of adsorption is high, the catalyst surface is covered frontwise. When the amount of adsorbate supplied from the gas phase is insufficient to bring about complete surface coverage, nonuniform coverage results.

INTRODUCTION

Temperature-programmed desorption (TPD) is a technique often used to obtain information on surface characteristics of porous catalysts, e.g., surface area, activation energy of desorption, and mechanism of desorption (*1, 2*). Although the experimental technique is rather simple, the theoretical complexity involved in TPD means that experimental studies commonly do not fully exploit the information present in TPD spectra.

In a few recent studies a theoretical analysis of TPD from porous catalysts has been presented (*3–6*). In these studies a mathematical model of the system is formulated and the resulting nonlinear differential equations describing the mass balances (with imposed initial and boundary conditions) are solved numerically. Such studies offer the possibility of obtaining insight into the effect of a change in a single experimental parameter. Thus, quantitative comprehension of TPD spectra is acquired. Various authors reported on the effect of carrier gas flow rate, carrier gas composition, catalyst pellet size, catalyst bed volume, and nonuniform initial coverage on desorption from porous supported metal catalysts (*4–6*). However, one should note that, given the derived set of differential equations, relations between the involved parameters are imposed. Gorte has properly analyzed these relationships in terms of four dimensionless groups (*3*). From the above model studies, it was also concluded that gas readsorption markedly affects the rate of desorption in porous systems. Adsorption equilibrium was found to be approached very closely throughout the course of TPD, when usual parameter values were substituted.

Model studies can also be used to test the applicability of techniques to estimate parameters on the basis of TPD information. Generally, these techniques do not take

[1] Present address: Philips Lighting B.V., P.O. Box 80020, 5600 JM Eindhoven, The Netherlands.

[2] Academic Computer Center Utrecht, Budapestlaan 8, Utrecht, The Netherlands.

0021-9517/89 $3.00

into account the mass transfer effects occurring in porous catalysts. When such an estimation method is applied to simulated spectra, comparison of the calculated value for a particular parameter with the model input value yields information on the applicability of the method. Rieck and Bell tested the heating rate variation technique in this way (*4*). The latter technique is applied to acquire values for the heat of adsorption and the preexponential factors for adsorption and desorption, provided adsorption is not activated (*1, 2*). The heat of adsorption appeared to be only slightly overestimated (about 5%). As might be anticipated from the equation for the rate coefficient, the values obtained for the preexponential factors deviated considerably from the input values (at least 200%).

The above-mentioned results were obtained from model calculations based on Langmuir adsorption and desorption kinetics (*7*). Although these assumptions are generally used in model studies, they have at least one serious drawback; i.e., the heat of adsorption is taken to be independent of the surface coverage. However, this does not agree with a multitude of experimental results.

A number of catalyst characterization techniques are based upon adsorption phenomena. The distribution of the adsorbate over the internal surface of the catalyst may strongly affect the experimental results. Obviously, the mathematical description for adsorption is analogous to that for desorption. Hence, the model used for the description of temperature-programmed desorption can be adapted easily to the case of adsorption.

A more fundamental aspect of models describing adsorption and desorption in porous catalysts lies in the possibility to relate intrinsic kinetic parameters obtained on single crystals with results obtained on porous catalysts. The understanding of catalytic behaviour will be improved when the intrinsic kinetic parameters and transport phenomena occurring in porous systems are accounted for in a single model.

The present paper deals with the following:

(i) The models formulated elsewhere are extended in order to calculate TPD profiles with a coverage-dependent heat of adsorption. The thus calculated profiles will be compared with the profiles predicted if the heat of adsorption is taken to be constant.

(ii) The applicability of some techniques used for the determination of the heat of adsorption and the order of the desorption reaction, such as heating rate variation, desorption rate isotherm, skewness parameter analysis, peak width analysis, and shape index analysis, will be discussed in terms of the coverage dependence of the heat of adsorption.

(iii) The distribution of the adsorbate, which is realized when a porous catalyst is exposed to a limited amount of adsorbate, is investigated. The results obtained are discussed in relation to measurements of the magnetization at low magnetic field strength (*8*) for the case of some superparamagnetic supported catalysts.

(iv) Finally, the present authors hope to provide sufficient data on the mathematical procedures for others to be able to duplicate the calculations. Unfortunately, previous papers report only rather sparse details on the mathematical computation methods.

THEORY

In this section a model describing either a temperature-programmed desorption experiment or an adsorption experiment is presented. The process is taken to occur in a packed bed of spherical catalyst pellets. The adsorbate is swept out of the reactor into a flow of an inert carrier gas or into a vacuum.

The following assumptions have been made:

(i) The gas phase in the void volume of the reactor bed is perfectly mixed, i.e., no axial or radial concentration gradients are present. Thus, the bed can be treated as a

single continuously stirred tank reactor (CSTR). When analysis reveals that the bed should be described in terms of a number of CSTRs connected in series, the model may be extended (*4*, *9*).

(ii) No temperature gradients are present in the catalyst bed. The gas-phase temperature equals the temperature of the solid phase.

(iii) External mass transfer effects are negligible. This implies that the concentration of reactants and products at the exterior surface of each catalyst pellet equals the concentration in the gas phase.

(iv) Within the pores inside a catalyst pellet, transport is only brought about by diffusion. Convection is considered to be insignificant.

(v) Reactions between adsorbate molecules or between adsorbate and adsorbent, such as disproportionation of CO or formation of volatile carbonyls, do not proceed.

(vi) Lag times due to detector and thermocouple response are neglected.

The formulas in this paper resemble essentially the equations that have been analyzed elsewhere. We prefer to adopt mainly the nomenclature presented by Rieck and Bell (*4*). Definitions of the symbols appearing in the following equations are given in Appendix 1.

The temperature increases linearly according to

$$T(t) = T_0 + \beta t. \tag{1}$$

The volumetric flow rate, Q, is given by

$$Q = Q_0\, T/T_0 \qquad \text{(inert carrier gas)} \tag{2a}$$

$$Q = Q_0\, (T/T_0)^{0.5} \qquad \text{(vacuum)}. \tag{2b}$$

Assuming Langmuir adsorption behavior, the net rate of desorption from adsorption sites is given by

$$\frac{\delta\theta}{\delta t} = \alpha k_a C_p (1 - \theta)^\alpha - \alpha k_d \theta^\alpha. \tag{3}$$

The terms on the right-hand side express the rates of adsorption and desorption. The order of adsorption (α) is taken to be equal to the order of desorption. For nondissociative adsorption this order is unity; for dissociative adsorption it equals two. Note that both C_p and θ are functions of the radial position within a catalyst pellet.

According to the kinetic theory of gases the rate coefficient for adsorption (k_a) can be written as

$$k_a = s_0 (RT/2\pi M)^{0.5} \sigma \tag{4}$$

The rate coefficient for desorption from a single adsorption site is given by

$$k_d = k_d^0 \exp(-E_d/RT) \tag{5}$$

The above equations imply that adsorption is assumed to be not activated; i.e., the heat of adsorption is equal to the activation energy for desorption. As the heat of adsorption is known to depend on the fraction of the surface covered with adsorbate, the activation energy for desorption is taken to decrease with increasing coverage according to

$$E_d = E_d^{\max} - (E_d^{\max} - E_d^{\min})\theta^x. \tag{6}$$

In this equation the exponent x can be adapted to approach experimentally observed behavior.

Within each catalyst pellet the following material balance can be derived:

$$\frac{\delta C_p}{\delta t} = \frac{D_e}{\varepsilon_p} \frac{1}{r^2} \frac{\delta}{\delta r} \left(r^2 \frac{\delta C_p}{\delta r} \right) - \frac{\rho_s}{\alpha \varepsilon_p} \frac{\delta \theta}{\delta t}. \tag{7}$$

The first term on the right-hand side of this equation represents the change in the gas-phase concentration due to the radial molecular diffusive flux of adsorbate. The second term describes the change in the partial pressure, brought about by desorption from adsorption sites. Applying the random-pore model the effective diffusion coefficient (D_e) is given by

$$D_e = D_k \varepsilon_p^2 = \tfrac{2}{3}(8RT/\pi M)^{0.5} a_p \varepsilon_p^2. \tag{8}$$

Note that this expression should contain the pore radius a_p, instead of the pore diameter as mentioned elsewhere (*4*).

The solution of the above set of nonlinear partial differential equations asks for speci-

fication of both the initial conditions and the boundary conditions. The boundary conditions defined at the border of the catalyst pellets are of the type "integro-differential" (*10*) and arise frequently in the study of mass transfer through a boundary layer.

The initial conditions ($t = 0$) are

$$C_p = 0 \quad \text{(for all } r\text{, except } r = R_p) \tag{9}$$

$$C_b = C_b^{init} \quad \text{(in the case of desorption } C_b^{init} = 0). \tag{10}$$

The boundary conditions are

$$(\delta C_p/\delta r) = 0 \quad (r = 0) \tag{11}$$

$$C_p = C_b \qquad (r = R_p). \tag{12}$$

As external mass transfer effects were taken to be absent, the concentrations in the effluent gas equal the gas-phase concentrations at the exterior surface of the catalyst pellets.

The integro-differential boundary condition specifies the supply and removal of adsorbate by convection and the diffusive flux through the exterior surface of the catalyst pellets,

$$\frac{\delta C_b}{\delta t} = \frac{Q_0 C_b^{init}}{V\varepsilon_b} - \frac{QC_b}{V\varepsilon_b} - \frac{3D_e}{R_p}\frac{(1-\varepsilon_b)}{\varepsilon_b}\frac{\delta C_p}{\delta r}\bigg|_{r=R_p}. \tag{13}$$

The first term equals zero except for the case of adsorption from a gas flow containing the adsorbate.

The numerical method used for solving the set of differential equations given above is described in Appendix 2.

RESULTS AND DISCUSSION

Desorption

The parameters used in the TPD simulations are listed in Table 1. The catalyst properties and the parameters describing the adsorption and desorption kinetics are representative for supported Group VIII metal catalysts. Also indicated in the table

TABLE 1

Parameter Values Used for the Simulations

R_p	0.02 cm	M	28 g/mol
a_p	$1.0\ 10^{-6}$ cm	s_0	0.5
ε_b	0.40	k_d^0	10^{15} s^{-1}
ε_p	0.70	E_d	30 kcal/mol or 30–10 θ kcal/mol
ρ_s	$9.77\ 10^{-5}$ mol/cm^3	α	1
σ	$4.03\ 10^8$ cm^2/mol	Q_0	1.0–1000.0 cm^3/s
V	0.063 cm^3	β	0.1–5.0 K/s
		T_0	298 K

are the ranges examined for the mass flow rate and the heating rate. Only first-order adsorption and desorption kinetics are discussed here.

Benzinger and Madix have studied thermal desorption of carbon monoxide from an Fe(100) surface (*11*). These authors observed four different desorption maxima, peaking at 250, 340, 430, and 800 K. The state desorbing at 800 K is attributed to dissociated carbon monoxide molecules. We do not consider the desorption of dissociatively adsorbed carbon monoxide. Since we assume the previous adsorption to be carried out at room temperature, we also do not consider the adsorption proceeding below about 300 K. We assume that in our desorption procedure only the molecularly adsorbed carbon monoxide desorbing from about 300 to 450 K is involved. The isosteric heat of the molecular adsorption of CO on iron (at 298 K) is reported to vary from about 30 kcal/mol at zero coverage to about 20 kcal/mol at full coverage (*12*). The experimentally observed behavior was approached assuming a linear rise of the activation energy for desorption from 20 to 30 kcal/mol as θ decreases from full to zero coverage. In addition, calculations were performed assuming a constant activation energy of desorption of 30 kcal/mol. This was done to gain insight into the effect of the coverage dependence of the activation energy for desorption and to facilitate comparison with results reported elsewhere.

The effect of variation of the activation

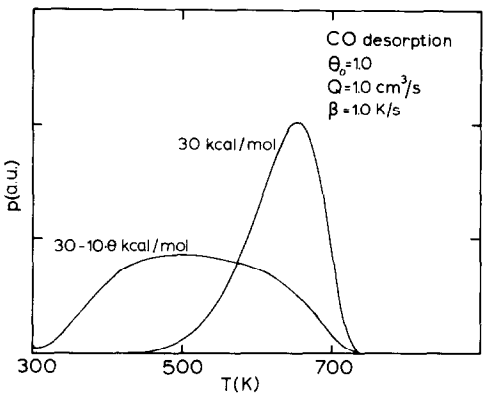

FIG. 1. Effect of the coverage dependence of the heat of adsorption on TPD profiles. The maximum pressure for the constant activation energy profile corresponds to 180 Pa. The pressures indicated refer to room temperature concentrations (as actually detected, e.g., with thermal conductivity detectors).

energy with fractional coverage is shown in Fig. 1 for a carrier gas flow rate (Q_0) of 1.0 ml/s, a heating rate (β) of 1.0 K/s, and a uniform initial coverage (θ) of 1.0. Under these conditions adsorption equilibrium is closely approached. The curve obtained for the constant activation energy of 30 kcal/mol is in good agreement with results presented by Rieck and Bell (*4*), when it is taken into account that their results refer to the gas-phase concentrations at the actual desorption temperature, while the results presented here refer to pressures at room temperature. In the case of the smaller initial activation energy a rapid initial rise of the pressure, due to the establishment of the equilibrium pressure, is observed. The small activation energy for desorption at full surface coverage causes the amount of adsorbate desorbing at low temperatures to be relatively large. The maximum desorption rate is reached at lower temperatures and at higher surface coverages than in case of a constant (maximal) activation energy. Also, the peak width is increased and the asymmetrical shape, typical for first-order processes with a constant activation energy, is not observed. This implies that skewness parameter analysis, a method to determine the order of the desorption reaction from a parameter calculation on the basis of symmetry of the peak, cannot be used when the adsorption energy varies with the surface coverage. Peak width analysis, in which the activation energy for desorption is obtained from the full peak width at one-half or at three-quarters of the maximum amplitude, is not valid either, since the coverage dependence of the activation energy largely affects the peak width. Also, shape index analysis is applicable only in the case of a constant activation energy. This method uses the shape index, which is defined as the ratio of the slopes at the inflection points of a single TPD curve, to determine the order of desorption and the presence of readsorption. These slopes depend on the magnitude of the activation energy and therefore their ratio will be influenced by a variation of this energy during the course of TPD. The above-mentioned methods are described more extensively elsewhere (*2*).

Figure 2 presents spectra obtained on varying the uniform initial coverage. At decreasing initial coverage the peak maximum is shifted to higher temperatures. In the case of a coverage-dependent activation energy for desorption this shift is only partly explained by an increased rate of readsorption, due to the larger fraction of unoccupied sites. There is also a contribution from the smaller rate coefficient for desorption, caused by the higher activation energy for desorption at low surface coverage. This causes the TPD spectra for different initial coverages to coincide at lower temperatures and higher surface coverages than in the case of a constant heat of adsorption.

The effect of a change in the rate of mass transfer (due to either a flow of inert gas or vacuum pumping speed) and the effect of a change in the heating rate are as could be anticipated from results reported elsewhere (*4, 5*). At high mass flow rates large intraparticle concentration gradients are present. For a heating rate of 1.0 K/s and full initial surface coverage the ratio $C_p(r =$

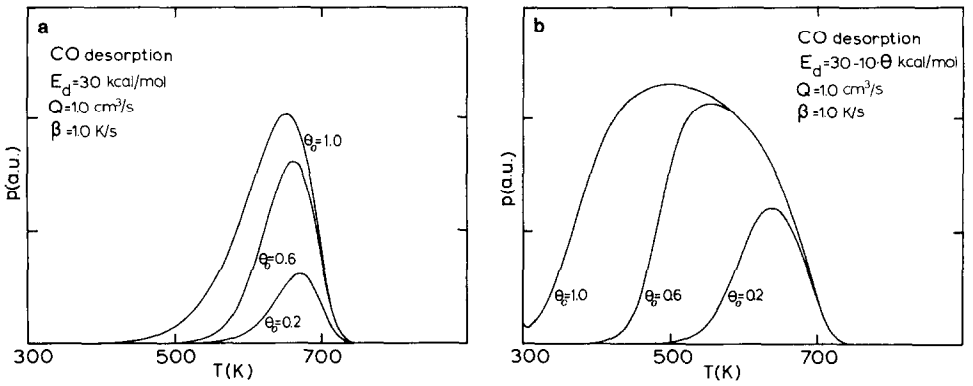

FIG. 2. Effect of the initial coverage on TPD profiles. (a) Constant heat of adsorption, (b) coverage-dependent heat of adsorption. Note the coincidence of the curves at the high-temperature flank in case (b).

0)/C_b equals 1.03 at a flow rate of 1.0 cm³/s, whereas it equals 92 at a vacuum pumping speed of 1000 cm³/s.

The heating rate variation technique is often applied to obtain the heat of adsorption from measured TPD spectra (*1, 2*). The heat of adsorption is obtained from the slope of a plot of $\ln(\beta/T_p^2)$ versus $(1/T_p)$, referred to as $E_d(\beta/T_p^2)$, or from the slope of a plot of $\ln(N_p)$ versus $(1/T_p)$, referred to as $E_d(N_p)$. The results for various sets of experimental conditions are listed in Table 2. Irrespective of the initial coverage, the heat of adsorption is estimated within 10% when the heat of adsorption is constant. If the activation energy for desorption used for the calculation of the spectra varies with the surface coverage, the heat of adsorption obtained using the heating rate variation technique strongly depends on the initial surface coverage. The rate of mass transfer and thus the presence of intraparticle concentration gradients appear to be of minor importance. The data given in the table show that application of the heating rate variation method to a series of TPD profiles obtained at different uniform initial coverages results in a rough indication of the variation of the heat of adsorption with the surface coverage.

TABLE 2

Values of the Heat of Adsorption Determined by Applying the Heating Rate Variation Method

E_d^{input} (kcal/mol)	θ_0	Q_0 (cm³/s)	$E_d(\beta/T_p^2)$	$E_d(N_p)$
30	1.0	1.0	31.0 ± 0.3	31.0 ± 0.2
	1.0	1000.0	30.5 ± 1.5	30.5 ± 1.4
	0.2	1.0	32.5 ± 1.1	32.5 ± 1.1
	0.2	1000.0	29.3 ± 1.2	29.4 ± 1.2
30–10 θ	1.0	1.0	22.1 ± 0.7	22.9 ± 0.7
	1.0	1000.0	23.6 ± 0.6	24.2 ± 0.6
	0.6	1.0	25.3 ± 0.7	26.1 ± 0.7
	0.6	1000.0	25.6 ± 0.7	26.2 ± 0.7
	0.2	1.0	27.9 ± 1.1	28.5 ± 1.1
	0.2	1000.0	28.3 ± 0.2	28.6 ± 0.2

Note. Heating rates of 0.1, 1.0, and 5.0 K/s were used for the calculations of the TPD profiles. Errors correspond to errors in the least-squares approximation.

Another method used to estimate the heat of adsorption is the desorption rate isotherm method (*2*). A series of TPD profiles obtained for various initial coverages must be analyzed. Each point of a desorption curve corresponds to a desorption rate (N_s) at a given temperature (T_s) and surface coverage (θ_s). The area under the TPD curve above T_s yields the surface coverage. Determining N_s and θ_s at T_s for spectra with different initial coverages and plotting $\ln(N)$ versus $\ln(\theta/(1-\theta))$ (the desorption rate isotherm) gives the order of desorption (α). From a series of such desorption rate isotherms, plots of $\ln(N)$ versus $(1/T)$ can be obtained at a fixed coverage. The activation energy for desorption is obtained as a func-

TABLE 3

Values of the Heat of Adsorption Determined by Applying the Desorption Rate Isotherm Method

E_d^{input} (kcal/mol)	θ	$E_d^{expected}$	$E_d^{determined}$
30	0.20	30.0	30.2 ± 0.2
	0.27	30.0	30.4 ± 0.2
	0.40	30.0	30.4 ± 0.2
	0.60	30.0	30.2 ± 0.2
30–10 θ	0.08	29.2	28.4
	0.12	28.8	27.6
	0.20	28.0	28.4 ± 0.4
	0.27	27.3	27.4 ± 0.2
	0.35	26.5	27.6 ± 1.2
	0.57	24.3	26.2
	0.80	22.0	21.8

Note. TPD profiles were calculated for initial coverages of 1.0, 0.6, and 0.2 in the case of the constant activation energy. Initial coverages of 1.0, 0.9, 0.8, 0.7, 0.6, 0.5, 0.4, 0.3, 0.2, and 0.1 were used in the case of the coverage-dependent activation energy. When no error is reported only two data could be used in the least-squares approximation.

tion of the surface coverage from the slope of these plots. The results are listed in Table 3. The heat of adsorption is estimated with good accuracy when it is independent of the surface coverage. If the heat of adsorption varies with the surface coverage, a reasonable indication of the relationship between heat of adsorption and surface coverage is obtained. The inaccuracy is not due to theoretical failing, but can be traced back to the coincidence of TPD profiles for different initial coverages at the high-temperature edge. This means that the $\ln(N)$ versus $(1/T)$ plot is confined to a small number of data in a limited temperature range, causing large errors in the least-squares estimation of the slope.

Adsorption

Adsorption experiments were also simulated using the data listed in Table 1. The initial adsorbate pressure in the interparticle gas phase is represented by $C_p(r = R, t = 0)$, the adsorbate concentration at the edge of the catalyst pellets. It is assumed that the surface coverage and the adsorbate pressure in the pores initially equal zero. Two types of adsorption experiments can be distinguished, viz. dynamic adsorption (the adsorbate is present in a gas flow passed through the reactor) and static adsorption (the catalyst is exposed to an amount of adsorbate present in a fixed volume).

In the case of dynamic adsorption it is observed that adsorption occurs as a front, which gradually penetrates the catalyst pellets (Fig. 3). The front is caused by the high rate of adsorption, whereas the rate of desorption at room temperature is small, due to the large heat of adsorption (varying from 30 to 20 kcal/mol). When the supply of adsorbate is sufficiently large, the catalyst surface is completely covered within a relatively short time. Even in the case of adsorbate pressures in the inlet gas flow as low as 133 Pa the surface is saturated within 8 s.

When a partially covered surface is desired, adsorption should be performed under static conditions ($Q_0 = 0$ cm^3/s). Assuming a total volume of the catalyst bed of 1.0 cm^3, the solid catalyst volume (i.e., the catalyst volume including intraparticle pores, but excluding the interparticle void volume) equals 0.6 cm^3 for $\varepsilon_b = 0.4$. When the gas dosing volume is taken to be 600 cm^3 (a reasonable value for this kind of ex-

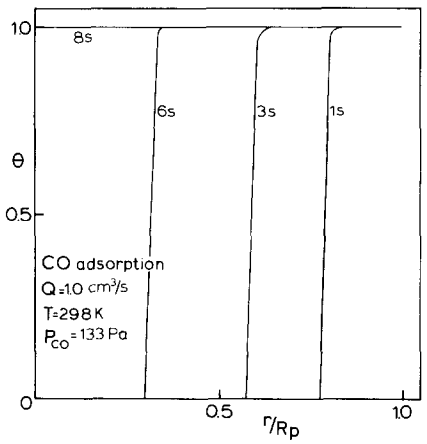

FIG. 3. Effect of the exposure time on the surface coverage in the case of dynamic adsorption.

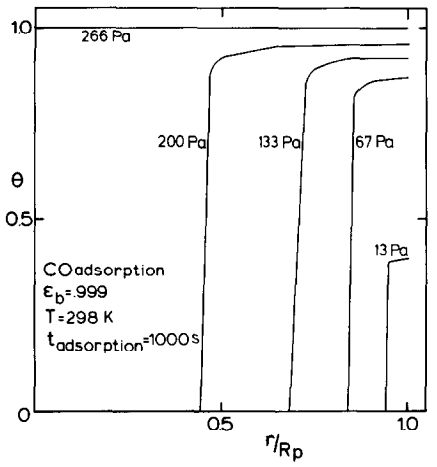

FIG. 4. Effect of the initial adsorbate pressure on the surface coverage in the case of static adsorption. The dosing volume is included in the catalyst bed void fraction.

periment), and assuming uniform adsorbate concentrations throughout the gas phase, this corresponds to an apparent catalyst bed void fraction of 0.999. Hence, in describing static adsorption ε_b was taken equal to 0.999; i.e., ε_b equals

$$\frac{\text{(gas dosing volume + interparticle volume)}}{\text{(gas dosing volume + interparticle volume + solid catalyst volume)}}.$$

The dosing volume is thus contained in the catalyst bed void fraction. The resulting surface coverage within the catalyst pellets after an exposure time of 1000 s is shown for a number of initial adsorbate pressures in Fig. 4. Figure 5 represents the surface coverage as a function of the exposure time for an adsorbate pressure of 133 Pa. As in the case of dynamic adsorption, the outer shells of the catalyst pellets are rapidly covered with adsorbate. When the amount of adsorbate in the gas phase is small, almost the entire amount of gas is adsorbed in a few seconds and a rapid large drop of the adsorbate pressure is noted. At room temperature the redistribution of adsorbate over the catalyst surface is very slow (Fig. 5), so a nonuniform surface coverage results. However, when the adsorption experiment is performed at a more elevated temperature, the surface coverage becomes more homogeneous (Fig. 6).

In the case of superparamagnetic catalysts (e.g., small particles of Ni, Fe, or Co), measurement of the magnetization at low magnetic field strength for different surface coverages yields the fraction of surface atoms relative to the total number of metal atoms (the dispersion of the metallic phase). The magnetization can be described by the Langevin equation for low magnetic field strength (Appendix 3). The dispersion is obtained from the plot of the relative magnetization (the ratio of the magnetiza-

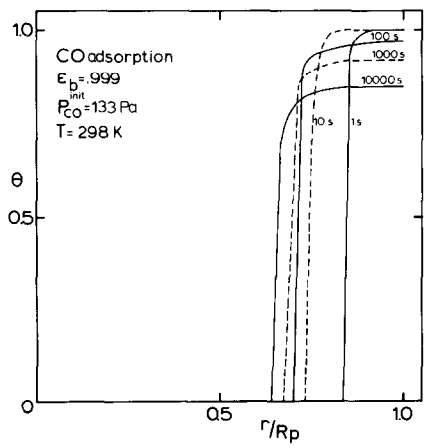

FIG. 5. Effect of the exposure time on the surface coverage in the case of static adsorption.

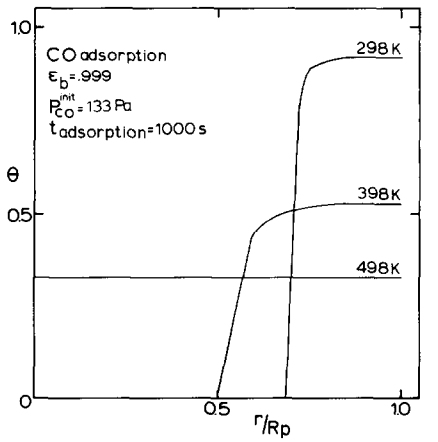

FIG. 6. Effect of the adsorption temperature on the surface coverage in the case of static adsorption.

TABLE 4

The Dispersion of the Catalyst as Calculated from Low-Field Magnetization Measurements for Homogeneous and Inhomogeneous Coverage of the Catalyst Surface, Respectively

n_a^{max}/n	Calculated dispersion	
	Homogeneous coverage	Inhomogeneous coverage
0.10	0.10	0.095
0.20	0.20	0.180
0.30	0.30	0.255
0.40	0.40	0.320

tion of the catalyst partly covered with adsorbate and the magnetization of the uncovered catalyst) versus the surface coverage. The initial slope of this curve is proportional to the dispersion. In Appendix 3 this is shown to be valid only in the case of a homogeneously covered catalyst surface. When the adsorbate is present at the edge of the pellets exclusively, the dispersion is systematically estimated to be too low (Table 4). It is seen that the error increases with increasing dispersion, that is with decreasing particle size. However, since dispersions exceeding 20% are rare, the dispersion is usually estimated with reasonable accuracy when using the Langevin low-field magnetization method.

CONCLUSIONS

(i) The coverage dependence of the heat of adsorption strongly influences the onset temperature of desorption, the desorption rate maximum, and the shape of the TPD profile. Therefore, a number of interpretation techniques are not applicable. Only the heating rate variation technique and the desorption rate isotherm method give insight into the relationship between heat of adsorption and surface coverage.

(ii) Adsorption proceeds frontwise when the net rate of adsorption is high. An inhomogeneous fractional surface coverage results when the amount of supplied adsorbate is not sufficient to cover the entire catalyst surface. A homogeneous fractional coverage can be obtained only by exposing the catalyst to the adsorbate at high temperatures.

APPENDIX 1: NOMENCLATURE

a_p average pore radius (cm)
C_b interparticle gas-phase concentration of adsorbate (mol/cm^3)
C_b^{init} adsorbate concentration in the inlet gas flow (mol/cm^3)
C_p intraparticle gas-phase concentration of adsorbate (mol/cm^3)
D_e effective diffusion coefficient (cm^2/s)
D_k Knudsen diffusion coefficient (cm^2/s)
E_d activation energy for desorption (kcal/mol)
E_d^{max} activation energy for desorption at zero coverage (kcal/mol)
E_d^{min} activation energy for desorption at full coverage (kcal/mol)
k_a rate coefficient for adsorption (cm^3/mol s)
k_d rate coefficient for desorption (s^{-1})
k_d^0 preexponential factor for desorption (s^{-1})
M molecular weight of adsorbate (g/mol)
m weight of catalyst (g)
N rate of desorption (mol/s)
N_p maximum rate of desorption (mol/s)
N_s rate of desorption at T_s (mol/s)
p adsorbate pressure (Pa)
Q volumetric mass flow rate at T (cm^3/s)
Q_0 volumetric mass flow rate at T_0 (cm^3/s)
R gas constant (kcal/mol K)
R_p pellet radius (cm)
r radial position within pellet (cm)
s_0 initial sticking coefficient
T temperature (K)
T_p temperature for which the desorption rate is maximal (K)
T_s specific temperature (K)
T_0 initial temperature (298 K)
t time (s)
V total volume of catalyst (cm^3)
x exponential factor for the coverage dependence of E_d

α order of reaction
β heating rate (K/s)
ε_b catalyst bed void fraction
ε_p catalyst pellet void fraction
θ fractional surface coverage
θ_p fractional surface coverage at T_p
θ_s fractional surface coverage at T_s
θ_0 fractional surface coverage at T_0
ρ_s concentration of adsorption sites (mol/cm^3)
σ area of adsorption site (cm^2/mol)

APPENDIX 2

The method used for solving the set of nonlinear partial differential equations is outlined briefly.

The distance from the center of the catalyst pellets ($r = 0$) to the outer edge of the pellets ($r = R_p$) is divided into N intervals $[R_{i-1}, R_i]$, with i varying from 1 to N, such that the following holds: $R_0 = 0$, $R_N = R_p$, $R_0 < R_1 < \cdots < R_N$. The results are within the acquired accuracy when the pellet radius was divided into 20 equidistant intervals; i.e., $N = 20$ and $R_i - R_{i-1} = R$ is constant. The program can easily be adapted to any number of intervals, which eventually may be taken nonequidistant.

All first- and second-order spatial derivatives, appearing in Eqs. (7) and (13), are estimated by expanding the functions in a Taylor series. The Taylor expansions were confined to the first three terms. In this way the first-order derivative of a function v at position x, $v'(x)$, can be approximated by expansion of $v(x + h_1)$ and $v(x - h_2)$:

$$v(x + h_1) = v(x) + h_1 v'(x) + (h_1^2/2)v''(x) + \cdots. \quad \text{(A-1)}$$

$$v(x - h_2 = v(x) - h_2 v'(x) + (h_2^2/2)v''(x) - \cdots. \quad \text{(A-2)}$$

By multiplying Eq. (A-1) by h_2 and Eq. (A-2) by h_1 and subtracting the thus obtained equations, an approximation for $v'(x)$ is obtained in terms of $v(x)$, $v(x + h_1)$, $v(x - h_2)$, h_1, and h_2:

$$v'(x) = [h_2 v(x + h_1) - h_1 v(x - h_2) - \{h_2 - h_1\}v(x)]/2h_1h_2. \quad \text{(A-3)}$$

The second derivative can be obtained analogously and is represented by

$$v''(x) = 2[h_2 v(x + h_1) + h_1 v(x - h_2) - \{h_1 + h_2\}v(x)]/[h_1^2 h_2 + h_1 h_2^2]. \quad \text{(A-4)}$$

For $x = R_i$ and $h_1 = h_2 = \Delta R$ we obtain

$$v'(R_i) = [v(R_{i+1}) - v(R_{i-1})]/2\Delta R \quad \text{(A-5)}$$

$$v''(R_i) = [v(R_{i+1}) + v(R_{i-1}) - 2v(R_i)]/\Delta R^2. \quad \text{(A-6)}$$

Since $v(R_{N+1})$ does not exist, the first-order derivatives at the edge of the pellet are approximated by using a single Taylor series:

$$v(R_{N-1}) = v(R_N - \Delta R) = v(R_N) - \Delta R v'(R_N) + (\Delta R^2/2)v''(R_N) - \cdots \quad \text{(A-7)}$$

from which follows that

$$v'(R_N) = [v(R_N) - v(R_{N-1})]/\Delta R. \quad \text{(A-8)}$$

The above described spatial discretization of the system results in a set of nonlinear rigid ordinary differential equations (ODEs), used for the calculation of coverage and pressure at 20 shells within the catalyst pellet as a function of time. The time intervals at which the coverage and pressure had to be calculated depended on the rate at which the solution changed: at the start of the calculation, very small time intervals (10^{-9} s) were necessary. These intervals could be rapidly increased and after about 1 s of simulated desorption, intervals of the order of magnitude of 1 s could be chosen.

The set of differential equations has been solved using the integration routine LSODE (*13*). The time needed for the calculation of a single TPD profile was about 10 CPU seconds on a CDC CYBER 180/855 under NOS/BE.

APPENDIX 3

The magnetization at low magnetic field strengths of a ferromagnetic catalyst with uniform metallic particles, exhibiting superparamagnetism, is given by

$$M_0 = N_{fp} n^2 m^2 H/3kT. \quad \text{(B-1)}$$

N_{fp} is the number of ferromagnetic particles, n the number of atoms in a ferromagnetic particle, m the magnetic moment of a ferromagnetic atom, and H the magnetic field strength.

When it is assumed that n_a atoms at the surface of a ferromagnetic particle are magnetically decoupled upon adsorption of a probe molecule, the magnetization in the case of homogeneous adsorption is given by

$$M_a = N_{fp}(n - n_a)^2 m^2 H/3kT. \quad \text{(B-2)}$$

Thus the relative magnetization can be expressed as

$$M_a/M_0 = 1 - 2(n_a/n) + (n_a/n)^2. \quad \text{(B-3)}$$

Usually, M_a/M_0 is plotted versus n_a/n_a^{max}. Since n_a^{max} is the number of surface atoms magnetically decoupled at full surface coverage, n_a/n_a^{max} equals the fractional surface coverage θ. The initial slope of the plot of M_a/M_0 versus n_a/n_a^{max} is given by

$$\delta(M_a/M_0)/\delta(n_a/n_a^{max})\big|_{n_a=0} = -2(n_a^{max}/n). \quad \text{(B-4)}$$

The dispersion of the metallic phase (n_a^{max}/n) can be obtained from the initial slope of the plot of M_a/M_0 versus n_a/n_a^{max}.

However, when all the adsorbate is present at the edge of the catalyst pellets, the ferromagnetic particles at the center of the catalyst pellet are not covered at all, whereas the ferromagnetic particles at the edge are fully covered. When N_a is the number of ferromagnetic particles fully covered, the magnetization is given by

$$M_a = [(N_{fp} - N_a)n^2 m^2 H + N_a(n - n_a^{max})^2 m^2 H]/3kT. \quad \text{(B-5)}$$

The relative magnetization is

$$M_a/M_0 = 1 - 2(N_a/N_{fp})(n_a^{max}/n) + (N_a/N_{fp})(n_a^{max}/n)^2. \quad \text{(B-6)}$$

When comparing these two ways of adsorption, N_a/N_{fp} with nonuniform adsorption should equal n_a/n_a^{max} with uniform adsorption; i.e., in both cases the amount of adsorbate should be the same. Therefore Eq. (B-6) can be written as

$$M_a/M_0 = 1 - 2(n_a/n) + (n_a n_a^{max}/n^2) \quad \text{(B-7)}$$

and thus

$$\delta(M_a/M_0)/\delta(n_a/n_a^{max})/_{n_a=0} = -2(n_a^{max}/n) + (n_a^{max}/n)^2. \quad \text{(B-8)}$$

From the latter expression it is seen that the dispersion is systematically underestimated when the surface coverage is inhomogeneous.

ACKNOWLEDGMENT

These investigations were supported by the "Netherlands Foundation of Chemical Research" (SON) with financial aid from the "Netherlands Organization for the Advancement of Pure Research" (ZWO).

REFERENCES

1. Cvetanovic, R. J., and Amernomiya, Y., *Catal. Rev. Sci. Eng.* **6,** 21 (1972).
2. Falconer, J. L., and Schwarz, J. A., *Catal. Rev. Sci. Eng.* **25,** 141 (1983), and references therein.
3. Gorte, R. J., *J. Catal.* **75,** 164 (1982).
4. Rieck, R. J., and Bell, A. T., *J. Catal.* **85,** 143 (1984).
5. Herz, R. K., Kiela, J. B., and Marin, S. P., *J. Catal.* **73,** 66 (1982).
6. Jones, D. M., and Griffin, G. L., *J. Catal.* **80,** 40 (1983).
7. Tompkins, F. C., "Chemisorption of Gases on Metals," p. 94. Academic Press, London/New York, 1978.
8. Selwood, P. W., "Chemisorption and Magnetization," p. 74. Academic Press, New York, 1975.
9. Butt, J. B., "Reaction Kinetics and Reactor Design," Prentice-Hall, Englewood Cliffs, NJ, 1980.
10. Jensen, V. G., and Jeffreys, G. V., "Mathematical Methods in Chemical Engineering," p. 257. Academic Press, London/New York, 1963.
11. Benzinger, J., and Madix, R. J., *Surf. Sci.* **94,** 119 (1980).
12. Kock, A. J. H. M., and Geus, J. W., *Prog. Surf. Sci.* **20,** 165 (1985).
13. Hindmarsh, A. C., *ACM Signum Newslett.* **15,** 10 (1980).